Three-dimensional spin structure in exchange-biased antiferromagnetic/ferromagnetic thin films

R. Morales,[1,a] M. Vélez,[1] O. Petracic,[2] Igor V. Roshchin,[3] Z.-P. Li,[4] X. Batlle,[5]
J. M. Alameda,[1] and Ivan K. Schuller[4]

[1]*Departamento de Física, Universidad de Oviedo-CINN, 33007 Oviedo, Spain*
[2]*Institut für Experimentalphysik/Festkörperphysik, Ruhr-Universität Bochum, D-44780 Bochum, Germany*
[3]*Department of Physics, Texas A & M University, College Station, Texas 77843, USA*
[4]*Department of Physics, University of California-San Diego, La Jolla, California 92093, USA*
[5]*Departament de Física Fonamental and Institut de Nanociència i Nanotecnologia (IN2UB), Universitat de Barcelona, 08028 Barcelona, Spain*

A coexistence of lateral and in-depth domain walls in antiferromagnet/ferromagnet (AF/FM) thin films exhibiting double hysteresis loops (DHLs) is demonstrated. Comparison of single and DHLs together with local and global measurements confirms the formation of two oppositely oriented domains in the AF that imprint a lateral domain structure into the FM layer. Most significantly, the magnetization reversal mechanism within each opposite domain takes place by incoherent rotation of spring-like domain walls extending through the Ni thickness. Therefore, complex three-dimensional domain walls are created perpendicular and parallel to the AF/FM interface in exchange biased systems. © 2009 American Institute of Physics. [DOI: 10.1063/1.3216055]

The exchange interaction between antiferromagnetic (AF) and ferromagnetic (FM) thin films gives rise to a shift of the FM hysteresis loop along the magnetic field axis.[1] This is the main feature of exchange bias (EB)[2,3] but other effects such as enhancement of coercivity near the AF ordering temperature (T_N),[4–6] training,[7–10] and asymmetrical hysteresis loops below T_N are also attributed to EB.[10–14] In addition, the effect of EB on the magnetization reversal has important technological implications.[15–18] Most magnetic thin films reverse the magnetization by nucleation of opposite domains and propagation of domain walls perpendicular to the film plane.[19,20] However, in some AF/FM thin films, EB induces spring-like domain walls parallel to the AF/FM interface.[21–23] FeF$_2$/FM bilayers with low crystalline anisotropy display this latter kind of domain walls.[11,24] Additionally, epitaxial FeF$_2$/FM bilayers exhibit positive (negative) EB with high (low) cooling field (H_{FC}), i.e., single hysteresis loops with only one EB direction. A cooling field between these two regimens, an intermediate H_{FC}, yields double hysteresis loops (DHLs).[25] These DHLs arise from a bidomain state produced by a lateral distribution of magnetic domains with opposite EB sign.[26] In this work, we report on the spin structure and reversal mechanism of FeF$_2$/Ni bilayers that simultaneously present both in-depth and lateral (i.e., parallel and perpendicular to AF/FM interface) domain walls. We found that the incomplete domain walls observed in a *single* domain state[24] (low or high H_{FC}) are also created in a *bidomain* state (intermediate H_{FC}) yielding a complex three dimensional spin structure in the FM.

FeF$_2$ (100 nm)/Ni (21 nm) /Al (7.6 nm) thin films were grown on MgF$_2$ (110) single crystals by e-beam evaporation at a base pressure of 2×10^{-7} Torr. FeF$_2$ and Ni were deposited at a substrate temperature of 300 and 150 °C, respectively, and a rate of 0.05 nm/s. The bilayer was protected from oxidation by an Al layer. FeF$_2$ grows epitaxial in the (110) orientation, whereas Ni is polycrystalline with the easy axis lying in-plane along the [001] direction. The magnetic characterization was done using superconducting quantum interference device (SQUID) magnetometry and spatially resolved magneto-optical Kerr effect (MOKE).

The magnetic state of the sample at low temperature was established following two different protocols.[27] Protocol I: The Ni layer was demagnetized above the Néel temperature of FeF$_2$ $(T_N=78$ K). Figure 1(a) shows a demagnetization process at room temperature with a final remanence close to zero. Then the bilayer was cooled below T_N in zero field $(H_{FC}=0)$. Protocol II: The sample was cooled through the FeF$_2$ Néel temperature at an intermediate cooling field $(H_{FC} \neq 0)$, i.e., the one that yields a DHL. Both procedures lead to a DHL with the same negative and positive EB magnitude. Figures 1(b) and 2(a) show DHLs following protocols I and II, respectively, using MOKE illuminating the whole sample. The remanence, i.e., $M(H=0)$, of the DHL is determined either by the final remanence after demagnetization, in case of protocol I [Fig. 1(a)], or by the intermediate H_{FC} magnitude, in case of protocol II (see Fig. 1 in Ref. 26).

Although Figs. 1(b) and 2(a) are similar, the AF spin configuration that produces the two DHLs is significantly different as will be shown below. To investigate the magnetic domain configuration and the magnetization reversal mechanism, local, spatially resolved MOKE hysteresis loops were obtained for both cooling protocols. A 500 μm diameter focused laser was used for the local magneto-optical measurements.

Figure 1(c) shows nine MOKE hysteresis loops of the FeF$_2$/Ni bilayer at positions separated 1.5 mm in the sample plane. The loops are single and positively shifted in the lowermost row, and single and negatively shifted in the uppermost row. The magnetization curves in between correspond to DHLs. The color-coded background was generated from a contour plot calculated with the nine normalized remanences $[m_r=M(H=0)/M(H_{max})]$ of the loops. A position with 0
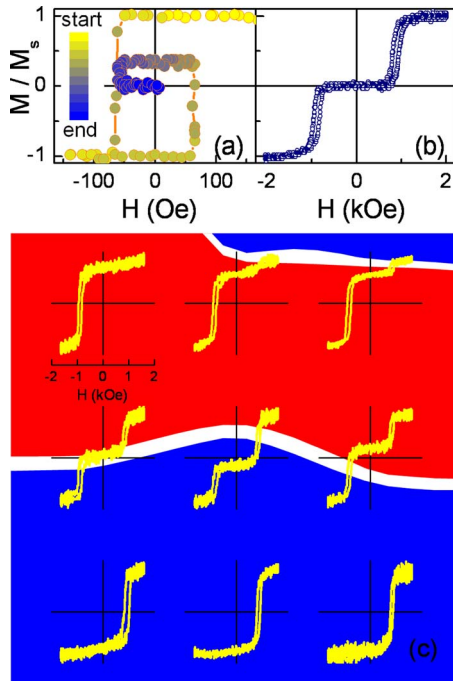
a)Electronic mail: rma@uniovi.es.

FIG. 1. (Color online) Protocol I. (a) Ni layer demagnetization at room temperature. (b) MOKE hysteresis loop at $T=20$ K illuminating the whole sample after cooling at the remanence set in (a). (c) Spatially resolved MOKE loops at nine positions. Color-coded background: red, domains yielding negative EB; blue, domains yielding positive EB; white, domain walls between opposite domains.

$< m_r \leq 1$ corresponds to an AF domain that yields negative EB (red color), while a remanence in the range $-1 \leq m_r < 0$ is produced by a domain with positive EB (blue color). The contour $m_r = 0$ separates opposite FM domains at $H=0$ and reflects the position of a AF domain wall (white color). DHLs arise as the laser spot probes an area with opposite
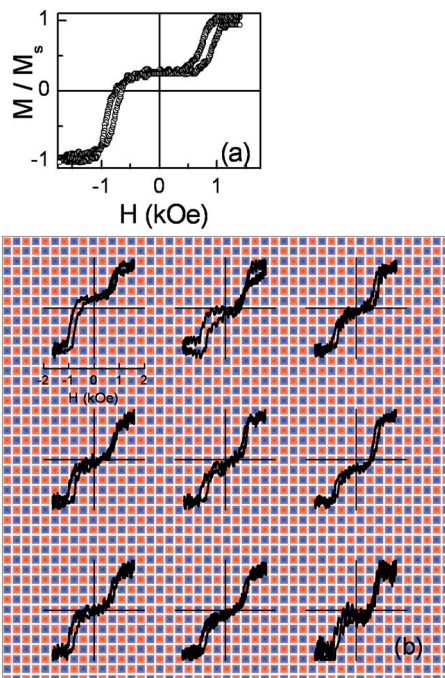

FIG. 2. (Color online) Protocol II. (a) MOKE loop at $T=20$ K illuminating the whole sample after cooling from room temperature at intermediate $H_{FC}=1$ kOe. (b) Spatially resolved MOKE loops at different positions. Illustrated color-coded background as in Fig. 1.

domains and the ratio of the two illuminated areas determines the remanence of the local magnetization curve. Figure 1(c) demonstrates that following protocol I the FM layer breaks up into a few, large magnetic domains during demagnetization. This lateral magnetic configuration is transferred into the AF layer during the cool down procedure below T_N. Once some of the AF spins become pinned, each AF domain exhibits only either negative (red) or positive (blue) EB.[27]

Figure 2(b) shows nine hysteresis loops at the same positions, as in Fig. 1(b). However, in this case the sample was warmed to room temperature and cooled to 20 K in $H_{FC} = 1$ kOe. All the local magnetization curves for protocol II are DHLs. These curves are the consequence of a bidomain state. During the cooling process at intermediate H_{FC}, the FM is positively saturated and the cooling field is high enough to break up the AF into opposite domains due to the local energy balance between the Zeeman term of AF uncompensated spins and the exchange energy of AF-FM moments at the interface.[28] The local DHLs demonstrate that the AF domains are much smaller in this case than those for protocol I. The laser spot cannot resolve separate domains, and probes a large number of domains with opposite sign of EB. This situation is schematically illustrated in Fig. 2(b) with a checkered background of small red and blue (negative and positive EB) domains. At remanence, $H=0$, the Ni magnetization splits into opposite domains resembling the underlying lateral AF structure. The domain size is much smaller than the laser spot since the remanence of all local DHLs is the same within experimental accuracy. Protocol II creates an intricate network of domain walls perpendicular to the AF/FM interface. These domain walls separate opposite exchange-biased domains.

In addition to the lateral configuration described above, the spin structure during the magnetization reversal is even more complex. The shape of DHLs implies the existence of in-depth magnetization profiles within each FM domain. The rounded approach to negative (positive) saturation of negative (positive) biased subloops in Fig. 1(b) (protocol I) is evidence of spring-like domain walls parallel to the AF/FM interface. It was demonstrated in Ref. 24 that this rounded approach in single hysteresis loops arises from incoherent rotation of domain walls extended through the FM thickness, i.e., the external field rotates the topmost FM spins which drag the spins underneath, creating a spring-like domain wall. This behavior is also observed in DHLs produced by protocol II. Figure 3(a) shows a DHL measured using SQUID magnetometry after cooling in $H_{FC}=1$ kOe. Figure 3(b) compares the rescaled negative biased subloop and a single loop obtained after a low cooling field ($H_{FC} = 0.5$ kOe, which induces negative EB single loops only) at the same temperature.[29] The two magnetization curves overlap and exhibit a rounded approach to negative saturation characteristic of parallel domain walls.[24] Therefore each AF domain formed upon cooling at intermediate H_{FC} produces the same reversal mechanism than that observed in single hysteresis loops, in which a spring-like domain wall is created through the thickness of the FM layer. Figures 3(c) and 3(d) illustrate the spin configuration during the magnetization reversal after protocol II. At remanence, $H=0$ [Fig. 3(c)], the FM layer splits into small opposite domains aligned with the AF easy axis. The FM spin configuration is a consequence of the AF coupling between AF-FM spins at the interface and resembles the AF domain structure created
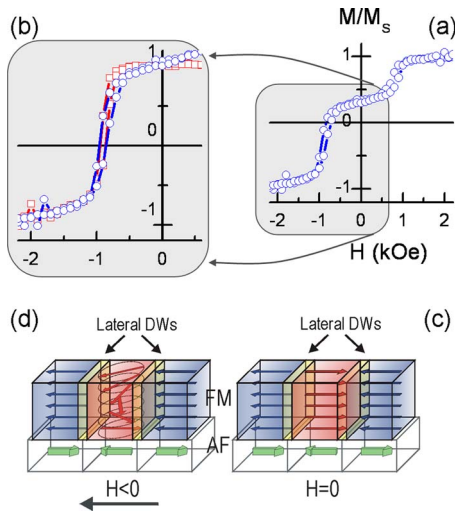
FIG. 3. (Color online) (a) DHL for intermediate $H_{FC} = 1$ kOe. (b) Comparison between a *single loop* (low $H_{FC} = 0.5$ kOe) (squares) and the rescaled *negative-biased subloop* from (a) (circles). Both loops were measured by SQUID at 10 K. (c) Illustrated spin configuration at $H=0$ and (d) $H<0$. Blue (left and right) and red (middle) domains yield positive and negative EB, respectively.

during the cooling process. The antiparallel AF-FM coupling is not frustrated and the configuration is stable but Néel walls are formed between positive and negative EB domains. At negative fields ($H<0$), the magnetization reversal of negatively biased domains (red) proceeds by incoherent rotation of Ni moments due to the strong coupling at the interface unlike in the case of a typical domain wall motion. Such a mechanism produces a rounded approach to negative saturation. On the other hand, the positively biased domains (blue) remain aligned with the negative field due to the favorable energetic situation, FM spins are parallel to the external field and antiparallel coupled to the AF. During this reversal, lateral domain walls (DWs) coexist with an in-depth magnetic profile within each negatively biased domain. Figure 3(d) illustrates this three-dimensional (3D) spin configuration for $H<0$ with a spring-like domain wall extending through the thickness of a negatively exchange-biased domain. Upon negative saturation both lateral and in-depth domain walls disappear and the exchange coupling in "red" domains is frustrated. Thus, reducing the field in the increasing branch of the subloop annihilates the spiral structure before zero field. Positive fields give rise to similar domain walls in positively exchange-biased domains (blue).

In conclusion, we have demonstrated the coexistence of both lateral and in-depth domain walls in AF/FM bilayers exhibiting DHLs. This 3D spin structure becomes complex upon cooling in intermediate fields H_{FC}. The finding elucidates the reversal mechanism of exchange-biased systems in a bidomain state and sheds light on the microscopic order of FM spins exchange coupled to an AF layer with opposite domains.

[1] W. H. Meiklejohn and C. P. Bean, Phys. Rev. **102**, 1413 (1956).
[2] M. Kiwi, J. Magn. Magn. Mater. **234**, 584 (2001).
[3] J. Nogues and I. K. Schuller, J. Magn. Magn. Mater. **192**, 203 (1999).
[4] C. Leighton, H. Suhl, M. J. Pechan, R. Compton, J. Nogues, and I. K. Schuller, J. Appl. Phys. **92**, 1483 (2002).
[5] M. Grimsditch, A. Hoffmann, P. Vavassori, H. T. Shi, and D. Lederman, Phys. Rev. Lett. **90**, 257201 (2003).
[6] R. Morales, Z. P. Li, J. Olamit, K. Liu, J. M. Alameda, and I. K. Schuller, Phys. Rev. Lett. **102**, 097201 (2009).
[7] A. Hoffmann, Phys. Rev. Lett. **93**, 097203 (2004).
[8] T. Gredig, I. N. Krivorotov, and E. D. Dahlberg, Phys. Rev. B **74**, 094431 (2006).
[9] U. Welp, S. G. E. te Velthuis, G. P. Felcher, T. Gredig, and E. D. Dahlberg, J. Appl. Phys. **93**, 7726 (2003).
[10] F. Radu, M. Etzkorn, R. Siebrecht, T. Schmitte, K. Westerholt, and H. Zabel, Phys. Rev. B **67**, 134409 (2003).
[11] Z.-P. Li, O. Petracic, R. Morales, J. Olamit, X. Batlle, K. Liu, and I. K. Schuller, Phys. Rev. Lett. **96**, 217205 (2006).
[12] A. Paul, E. Kentzinger, U. Rucker, and T. Bruckel, Phys. Rev. B **74**, 054424 (2006).
[13] J. Wang, W. N. Wang, X. Chen, H. W. Zhao, J. G. Zhao, and W. S. Zhan, Appl. Phys. Lett. **77**, 2731 (2000).
[14] M. R. Fitzsimmons, P. Yashar, C. Leighton, I. K. Schuller, J. Nogues, C. F. Majkrzak, and J. A. Dura, Phys. Rev. Lett. **84**, 3986 (2000).
[15] R. L. Stamps, J. Phys. D: Appl. Phys. **33**, R247 (2000).
[16] M. Kiwi, J. Mejia-Lopez, R. D. Portugal, and R. Ramirez, Europhys. Lett. **48**, 573 (1999).
[17] D. Mauri, H. C. Siegmann, P. S. Bagus, and E. Kay, J. Appl. Phys. **62**, 3047 (1987).
[18] M. D. Stiles and R. D. McMichael, Phys. Rev. B **59**, 3722 (1999).
[19] V. I. Nikitenko, V. S. Gornakov, A. J. Shapiro, R. D. Shull, K. Liu, S. M. Zhou, and C. L. Chien, Phys. Rev. Lett. **84**, 765 (2000).
[20] C. L. Chien, V. S. Gornakov, V. I. Nikitenko, A. J. Shapiro, and R. D. Shull, IEEE Trans. Magn. **38**, 2736 (2002).
[21] M. Kiwi, J. Mejia-Lopez, R. D. Portugal, and R. Ramirez, Appl. Phys. Lett. **75**, 3995 (1999).
[22] K. S. Lee, S. K. Kim, and J. B. Kortright, Appl. Phys. Lett. **83**, 3764 (2003).
[23] S. Roy, M. R. Fitzsimmons, S. Park, M. Dorn, O. Petracic, I. V. Roshchin, Z. P. Li, X. Batlle, R. Morales, A. Misra, X. Zhang, K. Chesnel, J. B. Kortright, S. K. Sinha, and I. K. Schuller, Phys. Rev. Lett. **95**, 047201 (2005).
[24] R. Morales, Z. P. Li, O. Petracic, X. Batlle, I. K. Schuller, J. Olamit, and K. Liu, Appl. Phys. Lett. **89**, 072504 (2006).
[25] J. Olamit, E. Arenholz, Z. P. Li, O. Petracic, I. V. Roshchin, R. Morales, X. Batlle, I. K. Schuller, and K. Liu, Phys. Rev. B **72**, 012408 (2005).
[26] O. Petracic, Z. P. Li, I. V. Roshchin, M. Viret, R. Morales, X. Batlle, and I. K. Schuller, Appl. Phys. Lett. **87**, 222509 (2005).
[27] I. V. Roshchin, O. Petracic, R. Morales, Z. P. Li, X. Batlle, and I. K. Schuller, Europhys. Lett. **71**, 297 (2005).
[28] Z. P. Li, R. Morales, and I. K. Schuller, Appl. Phys. Lett. **94**, 142503 (2009).
[29] MOKE loops of Fig. 2 are too noisy for this comparison. Moreover, magnetooptical measurements do not provide a quantitative value of the magnetic moment, which is obtained from SQUID measurements.